doi:10.1016/j.jmb.2012.02.042 J. Mol. Biol. (2012) 418, 181–196

Contents lists available at www.sciencedirect.com

Journal of Molecular Biology

journal homepage: http://ees.elsevier.com.jmb

Catalytic Versatility and Backups in Enzyme Active Sites: The Case of Serum Paraoxonase 1

Moshe Ben-David [1], Mikael Elias [2], Jean-Jacques Filippi [3], Elisabet Duñach [3], Israel Silman [4], Joel L. Sussman [1]* and Dan S. Tawfik [2]*

[1]*Department of Structural Biology, Weizmann Institute of Science, Rehovot 76100, Israel*
[2]*Department of Biological Chemistry, Weizmann Institute of Science, Rehovot 76100, Israel*
[3]*Laboratoire de Chimie des Molécules Bioactives et des Arômes, Université de Nice Sophia Antipolis—CNRS UMR 6001, Institut de Chimie de Nice, Parc Valrose, 06108 Nice Cedex 2, France*
[4]*Department of Neurobiology, Weizmann Institute of Science, Rehovot 76100, Israel*

Received 22 December 2011; received in revised form 19 February 2012; accepted 22 February 2012
Available online 1 March 2012

Edited by M. Guss

Keywords:
enzyme catalysis;
catalytic promiscuity;
enzyme promiscuity;
conformational diversity;
structural dynamics

The origins of enzyme specificity are well established. However, the molecular details underlying the ability of a single active site to promiscuously bind different substrates and catalyze different reactions remain largely unknown. To better understand the molecular basis of enzyme promiscuity, we studied the mammalian serum paraoxonase 1 (PON1) whose native substrates are lipophilic lactones. We describe the crystal structures of PON1 at a catalytically relevant pH and of its complex with a lactone analogue. The various PON1 structures and the analysis of active-site mutants guided the generation of docking models of the various substrates and their reaction intermediates. The models suggest that promiscuity is driven by coincidental overlaps between the reactive intermediate for the native lactonase reaction and the ground and/or intermediate states of the promiscuous reactions. This overlap is also enabled by different active-site conformations: the lactonase activity utilizes one active-site conformation whereas the promiscuous phosphotriesterase activity utilizes another. The hydrolysis of phosphotriesters, and of the aromatic lactone dihydrocoumarin, is also driven by an alternative catalytic mode that uses only a subset of the active-site residues utilized for lactone hydrolysis. Indeed, PON1's active site shows a remarkable level of networking and versatility whereby multiple residues share the same task and individual active-site residues perform multiple tasks (e.g., binding the catalytic calcium and activating the hydrolytic water). Overall, the coexistence of multiple conformations and alternative catalytic modes within the same active site underlines PON1's promiscuity and evolutionary potential.

Introduction

Enzyme promiscuity concerns the ability of a single active site to accommodate substrates other than the enzyme's native substrate—that is, the substrate for which an enzyme evolved (substrate ambiguity)—and/or catalyze reactions other than

**Corresponding authors.* E-mail addresses: joel.sussman@weizmann.ac.il; dan.tawfik@weizmann.ac.il.

Abbreviations used: PON1, paraoxonase 1; PDB, Protein Data Bank; 2HQ, 2-hydroxyquinoline.

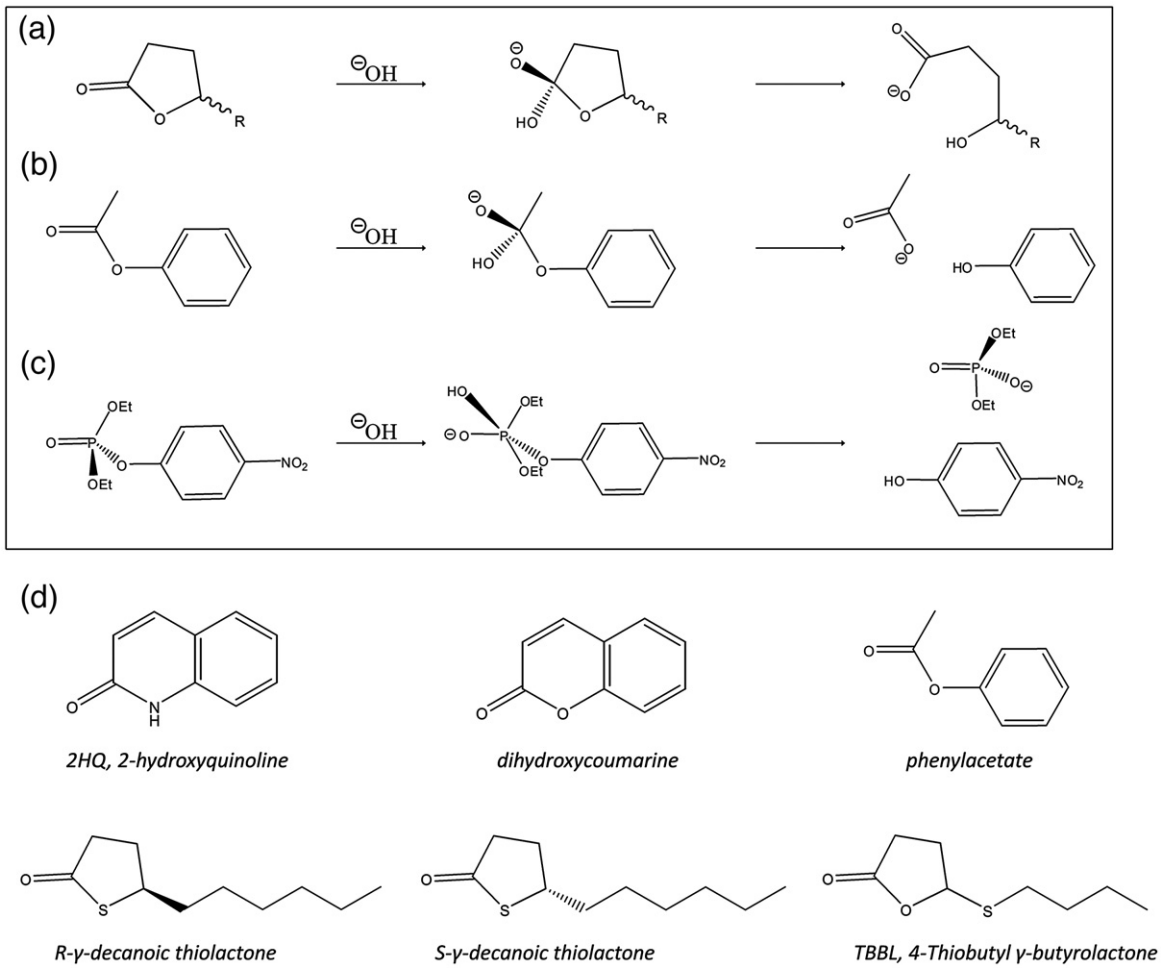

Fig. 1. General mechanisms for the hydrolysis of the three classes of rePON1 substrates: the lactones (a), the esters (b), and the phosphotriesters (c). The 2HQ inhibitor and additional substrate molecules are presented (d).

the native one (catalytic promiscuity). There are numerous examples of such phenomena, but there are only a few cases for which structural and mechanistic details are available.[1–6] In particular, we sought for a detailed description of the complexes and catalytic mechanisms for the native substrate of an enzyme and for its different alternative substrates and promiscuous reactions.

Our case study discusses the mammalian serum paraoxonase 1 (PON1). This enzyme comprises the most-studied member of a family of calcium-dependent hydrolases. As it turns out, the name paraoxonase relates to its promiscuous activity in hydrolyzing the phosphotriester pesticide paraoxon. PON1 is in fact a lactonase, and γ- and δ-lactones with long alkyl side chains (lipophilic lactones) are its most likely native substrates[7,8] (see also Refs. 9 and 10). The crystal structure of PON1 and of the first member of the serum paraoxonase family revealed a six-blade β-propeller fold with two calcium ions in its central tunnel.[11] The structural Ca^{2+} is buried, whereas the catalytic Ca^{2+} lies at the bottom of the active-site cavity. In the hydrolysis of lactones and aryl esters (C–O bond cleavages *via* tetrahedral intermediates; Fig. 1), a His115–His134 dyad deprotonates a water molecule to generate the attacking hydroxide, and the Ca^{2+} stabilizes the resulting tetrahedral oxyanionic intermediate.[12] However, the mode of promiscuous hydrolysis of phosphotriesters (P–O cleavage *via* a pentacovalent intermediate; Fig. 1) differs from that of lactones and aryl esters. This is clearly evident from the finding that mutations of His115 that diminish both the lactonase and aryl esterase activities actually enhance the rate of phosphotriester hydrolysis.[12,13] However, the structures of the various substrate and intermediate complexes and the origin of the differences in the modes of catalysis for lactones, esters, and phosphotriesters are unknown.

We aimed at an in-depth analysis of PON1's active site and a comparison of the different modes in

which it binds different substrates and catalyzes their hydrolysis. The previously published PON1 structure revealed the fold of PON1 and the key features of its active site.[11] However, the structure was determined at pH 4.5 where the enzyme is almost inactive. The absence of a structure with a ligand and the lack of density for the 'active-site loop' (residues 72–79, comprising the longest loop within the active site) also precluded a detailed description. Here, we describe the crystal structure of PON1 at pH 6.5, where the enzyme displays close to optimal activity, and of its complex with a lactone analogue. We also describe the kinetic characterization of mutants in the active-site loop and docking models of the various substrates and of their corresponding reaction intermediates.

Results

Structure of rePON1 at pH 6.5

As previously described, we utilized a recombinant PON1 variant, rePON1–G2E6 (herein referred to as rePON1), which is ~90% identical in sequence to both rabbit and human PON1s and exhibits the same enzymatic specificity.[14] The best crystals were obtained at pH 6.5 and diffracted to 2.0 Å resolution (Table 1). The structure obtained is overall identical with that of the first rePON1 structure obtained at pH 4.5 [2.2 Å; Protein Data Bank (PDB) ID: 1V04] and, as in the pH 4.5 structure, a phosphate ion is bound to the catalytic Ca^{2+}. However, the side chain of V346 within the active-site pocket is rotated relative to the pH 4.5 structure, and the side chains of F347 and H348 in the active-site's 'second shell' adopted completely different rotamers (Supplementary Fig. 1). Residues at the edges of the active-site loop, namely, residues 71, 80, and 81, which were ordered in the pH 4.5 structure, did not exhibit defined electron density at pH 6.5.

The complex with 2-hydroxyquinoline

The best known competitive inhibitor of PON1 is 2-hydroxyquinoline (2HQ).[8] In its tautomeric form, it is a lactam and therefore a non-hydrolyzable lactone analogue in which the esteric oxygen has been replaced by NH. The corresponding lactone, dihydrocoumarin, is hydrolyzed by rePON1 with $k_{cat}/K_m > 10^6$ M^{-1} s^{-1}.[8] 2HQ inhibits all three enzymatic activities of PON1 with a similar K_i (~2 μM).[8,15] Crystals diffracting to 2.2 Å were obtained by soaking 2HQ into the rePON1 crystals obtained at pH 6.5. The space group and unit cell parameters were very similar to those for the apo crystals (see Table 1). Structure determination was carried out by molecular replacement using the pH 6.5 rePON1 structure as the model.

Table 1. Summary of data collection and refinement statistics

	rePON1 at pH 6.5	2HQ/rePON1
Data collection		
Resolution range (Å)[a]	50–2.0 (2.03–2.0)	50–2.2 (2.24–2.2)
Space group	$P4_32_12$	$P4_32_12$
Unit cell dimensions (Å)		
$a=b$	93.653	93.5
c	143.703	144.6
Number of reflections measured	929,675	1,175,744
Number of unique reflections[a]	44,101 (2148)	33,798 (1666)
R_{sym}[a]	0.093 (0.53)	0.10 (0.62)
Completeness (%)[a]	99.3 (99.6)	100 (100)
Redundancy[a]	4.3 (4.2)	14.3 (14.4)
$\langle I\rangle/\langle\sigma(I)\rangle$[a]	15.8 (3.7)	31 (6)
Refinement statistics of the current models		
R_{free} (%)	22.02	22.49
R_{work} (%)	19.5	18.2
Water molecules	117	113
r.m.s.d.		
Bond length (Å)	0.015	0.031
Bond angles (°)	1.425	2.24
Ramachandran plot[b] (%)		
Favored	94.77	95.82
Allowed	100	99.7
PDB ID	3SRE	3SRG

[a] Values in parentheses are for the highest-resolution shell.
[b] Ramachandran plot statistics from MolProbity (http://molprobity.biochem.duke.edu).

The $F_o - F_c$ electron density map for the complex showed that 2HQ is bound to the catalytic calcium ion. Additional continuous density was revealed, matching the active-site loop, residues 71–81, most of which are not seen in the apo structures at either pH 4.5 or 6.5 (Fig. 2a). The phosphate ion that is bound to the catalytic calcium in both the apo structures is displaced by 2HQ. Further, 2HQ's carbonyl oxygen and NH moiety overlap with the phosphate oxygens in the apo structure (Fig. 2b). This overlap supports the notion that both the phosphate ion and 2HQ mimic the binding mode of substrates and/or reaction intermediates. The structured active-site loop provides a narrower active site and a larger interaction surface with 2HQ. Several loop residues that are disordered in the apo pH 6.5 structure contribute to the active-site wall in the complex (71–74; Fig. 2c). In contrast, residues 75–81 reside outside the active site. In addition to interacting with the catalytic calcium, 2HQ interacts with the side chains of H115, D269, E53, and N168 (Fig. 2d). Apart from the immobilization of the 71–81 loop, no significant changes were detected in PON1's backbone as a result of 2HQ binding.

The different rePON1 structures reveal the existence of various conformations that could refer to different conformational substates along the reaction coordinate and/or to different conformations that might be adopted upon binding of different

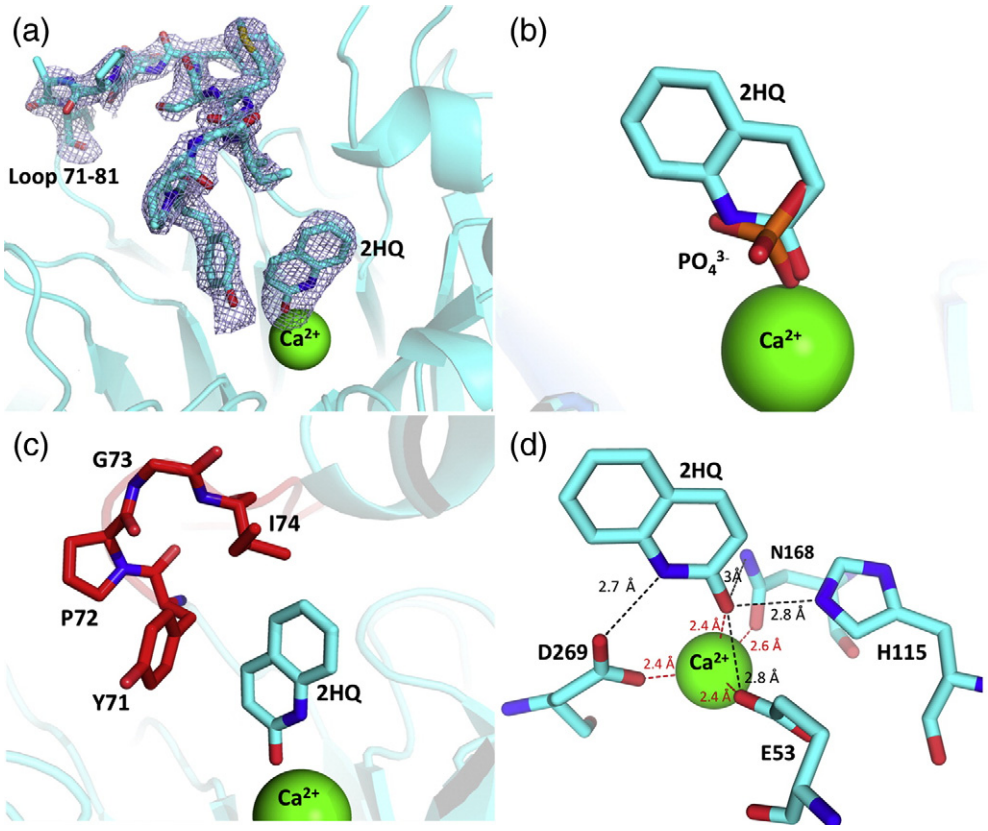

Fig. 2. Structural details of the 2HQ/rePON1 complex at pH 6.5. (a) 2HQ and the structured active-site loop in the rePON1/2HQ complex structure. The $F_o - F_c$ omit map is contoured at 3σ. (b) Overlay of the phosphate ion in the apo rePON1 at pH 6.5 and of 2HQ in the rePON1/2HQ complex. (c) The first segment of the active-site loop and residues Y71 and I74 in particular comprise part of PON1's active-site wall. (d) Interactions of 2HQ with active-site residues (interactions with the catalytic Ca^{2+} are highlighted in red).

substrates. Specifically, the bound 2HQ is in contact with the side chains of Y71 and I74 that point towards the binding site. However, in the absence of a ligand, Y71 is either disordered (pH 6.5) or positioned outside the binding pocket (pH 4.5; Fig. 3). Alignment of the three structures also shows that the orientation of V346, F347, and H348 side chains at pH 6.5 presents no steric hindrances with the active-site loop. However, in their orientations at pH 4.5, the side chains of F347 and H348 clash with the loop residues in the 2HQ complex. Indeed, the inward rotation of Y71 (as in the 2HQ complex) and the outward movement of F347 along with the rotation of its neighboring side chains V346 and H348 seem to be concerted (Fig. 3).

Overall, we identified three different conformations of rePON1: (i) The *closed conformation*, represented by the 2HQ complex structure, in which the active-site loop is structured and anchored to the enzyme's surface and Y71 points into the active site. (ii) The unbound conformation at pH 4.5, in which the active-site loop is flexible, but Y71 is fixed and points outside the active site. (iii) The unbound conformation observed at pH 6.5, in which the loop, including Y71, is flexible. The latter two are dubbed *open conformations*. These three conformations result in different pocket shapes and sizes (Fig. 4). As shown below, these different conformations provide different interaction potentials and mediate PON1's different catalytic activities.

Mutagenesis and kinetics

Ala mutants of residues 70–81 were characterized to further assess the role of the various loop conformations. Mutation of residues 71 and 74 that comprise part of the active-site wall and contact the lactone analogue 2HQ exhibited the strongest and most consistent effects on catalysis and on 2HQ binding (Fig. 5; Supplementary Tables 1–3). Of the loop residues that face the outer surface, residues 70 and 77 were the most affected by mutation to Ala, but the effects were much smaller than for residues 71 and 74. Certain mutants showed markedly different effects on different activities. For example, I74A resulted in a >20-fold decrease in the catalytic efficiency towards paraoxon and phenylacetate but had no effect on the lactonase activity. These data

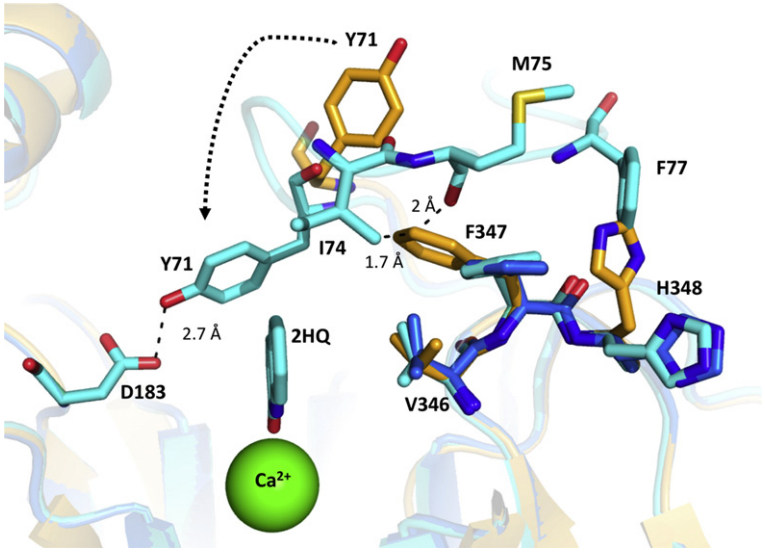

Fig. 3. Changes in the rePON1 binding site upon binding of 2HQ. Superimposition of the rePON1/2HQ complex (cyan; the *closed conformation*) with the apo rePON1 structures at pH 4.5 (orange) and pH 6.5 (blue) (the *open conformations*). The pH 4.5 conformation prevents closure of the active-site loop due to clashes of F347 and H348 with the loop residues (e.g., F77 and I74). Also illustrated is the movement of Y71 (dashed arrow) upon binding of 2HQ and its interaction with D183 in the 2HQ complex structure.

support the hypothesis that certain loop residues play a different role in the binding of different substrates and that different loop configurations are involved in binding and hydrolysis of different substrates. The Ala mutations affect k_{cat} much more than K_m, suggesting that the conformation of the active-site loop may be critical in stabilizing the transition state for catalysis and/or that a conformational change involving the loop (or individual loop residues) is associated with the catalytic turnover.

Modeling the substrate and reaction intermediates

We applied docking to assist the inference of the binding modes of PON1's different substrates and putative reaction intermediates (Fig. 1; Supplementary Fig. 2). Being aware of the limitations of docking, we assessed the validity of the docking models using a large number of PON1 mutants for which data concerning substrate specificity are available, as well as the stereoselectivity of lactone substrates examined here. Overall, computational docking was used to indicate potential modes of binding and catalysis, and, as specified below, the most likely models were chosen based on experimental data.

The docking procedure was first tested by modeling the inhibitor 2HQ into the open and the closed conformations, using the native structure at pH 4.5 and 6.5 for the open conformation and the 2HQ complex from which the 2HQ had been removed as the closed structure. As expected, the modeled conformation in the closed structure is essentially identical with that of the 2HQ complex obtained by X-ray crystallography. Furthermore, docking of 2HQ into the apo structures of PON1, at

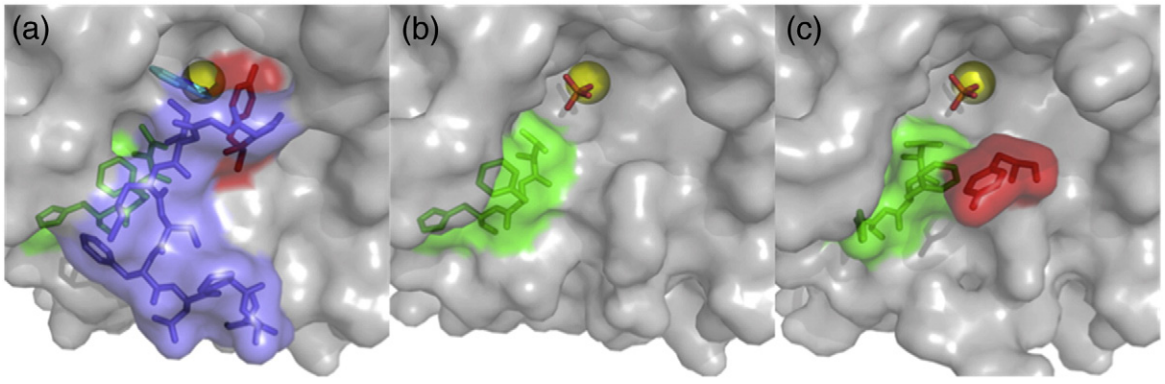

Fig. 4. Surface views of the different rePON1 active-site architectures in the three rePON1 structures. Highlighted are Y71 (red), residues 346–348 (green), and the active-site loop (light blue). (a) rePON1/2HQ complex (pH 6.5). (b) Apo rePON1 at pH 6.5. (c) Apo rePON1 at pH 4.5 (1V04).

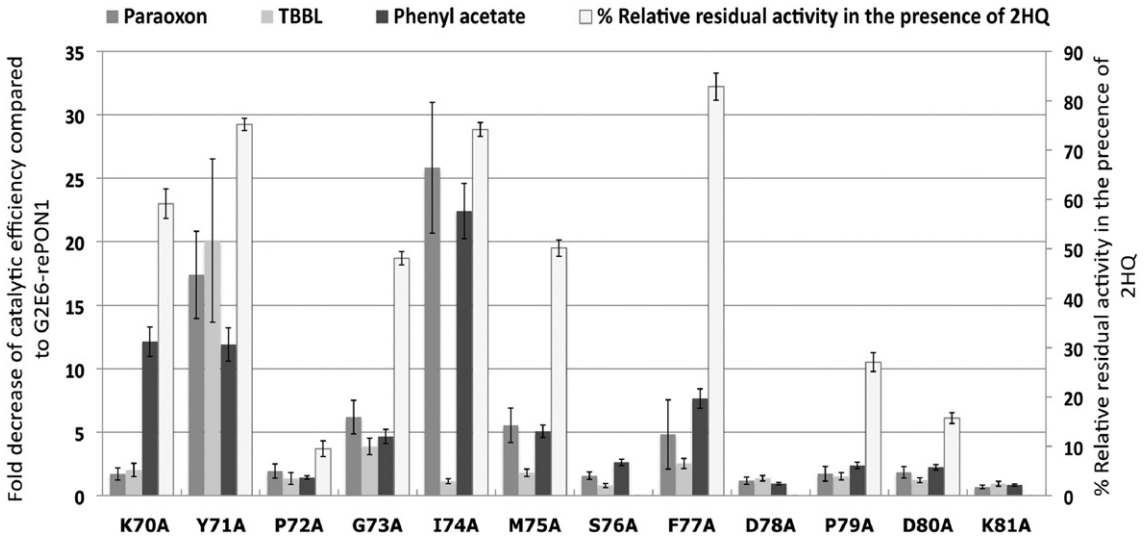

Fig. 5. Catalytic activity of PON1 mutants in which individual residues in the active-site loop had been mutated to Ala. Displayed are the fold decreases in catalytic efficiency (k_{cat}/K_m) relative to wild-type-like rePON1, for three different substrates. The chromogenic lactone substrate, TBBL, was used to measure lactonase activity; phenylacetate was used to measure aryl esterase activity, and paraoxon was used to measure phosphotriesterase activity (Fig. 1). Also shown (right *y*-axis) is the percentage residual paraoxonase activity in the presence of 25 μM 2HQ compared to rePON1 (29% residual paraoxonase activity at 25 μM 2HQ).

either pH 4.5 or 6.5 (the open conformation), yielded an identical binding mode (Supplementary Fig. 3). However, given that mutations in Y71 and I74, two loop residues that contact 2HQ only in the closed form (Fig. 3), significantly reduce 2HQ binding (Fig. 5), it is likely that 2HQ binds primarily to the closed form, as seen in the crystal structure (the closed form also shows preferable docking energy; Supplementary Table 4).

We subsequently modeled the structures of the complexes of PON1's characteristic native and promiscuous substrates. However, given that enzyme active sites are most complementary to the reaction's transition state, we primarily examined the models with the oxyanionic reaction intermediates that form upon nucleophilic attack on these substrates by hydroxide.[16] Since His115 was shown to act as a base for water activation in lactone and aryl ester hydrolysis,[12] and in the absence of evidence for an acyl or phosphoryl enzyme intermediate for any of the substrates tested (e.g., burst kinetics), we opted for water being the nucleophile (see Discussion).

Lipophilic lactones

γ- and δ-lactones with long-chain substituents appear to be the primary substrates of PON1.[7,8] Overall, the models obtained for the lactone's oxyanionic intermediates perfectly overlap with the 2HQ complex structure and also with the phosphate ion observed in the structure of the uncomplexed PON1 (Fig. 6a and b). Thus, the newly derived structure of the 2HQ complex is in agreement with our initial hypothesis that the phosphate ion reflects the binding mode of PON1's oxyanionic intermediates for aryl esters (e.g., phenylacetate; Fig. 6c)[11] and for lactones.[12] However, given the new structure, we were able to further refine the models and, thereby, to account for PON1's stereospecificity.

Indeed, although aliphatic lactones exhibit chirality at the γ/δ carbon, the stereoselectivity of PON1 has not been examined. The pH-indicator assay that is routinely used to monitor lactone hydrolysis permits measurements of initial rates but not of the entire reaction course.[8,15,17] We therefore used δ-decanoic thiolactone, in both its racemic and *S*-forms,[18] to follow the entire reaction course by monitoring thiol release with dithionitrobenzoic acid. Racemic δ-decanoic thiolactone exhibits a rapid phase of hydrolysis (~50% amplitude), followed by a second phase with an ~17-fold slower rate. The rate of hydrolysis for the *S*-isomer is ca 2-fold higher than that for the racemate, and the amplitude corresponds to 100% hydrolysis, indicating that the slow phase of racemate hydrolysis corresponds to the *R*-isomer (Fig. 7).

The docking models are consistent with the *R*- and *S*-isomers of δ-lactones binding in different modes (for both thio- and oxo-lactones, as well for δ- and γ-lactones). The ground states of *S*-lactones adopt a similar binding mode to that of 2HQ—the ester group superimposes both with 2HQ's lactam group and with the phosphate seen in the apo structure (Supplementary Figs. 4b and 5b). The lactone's

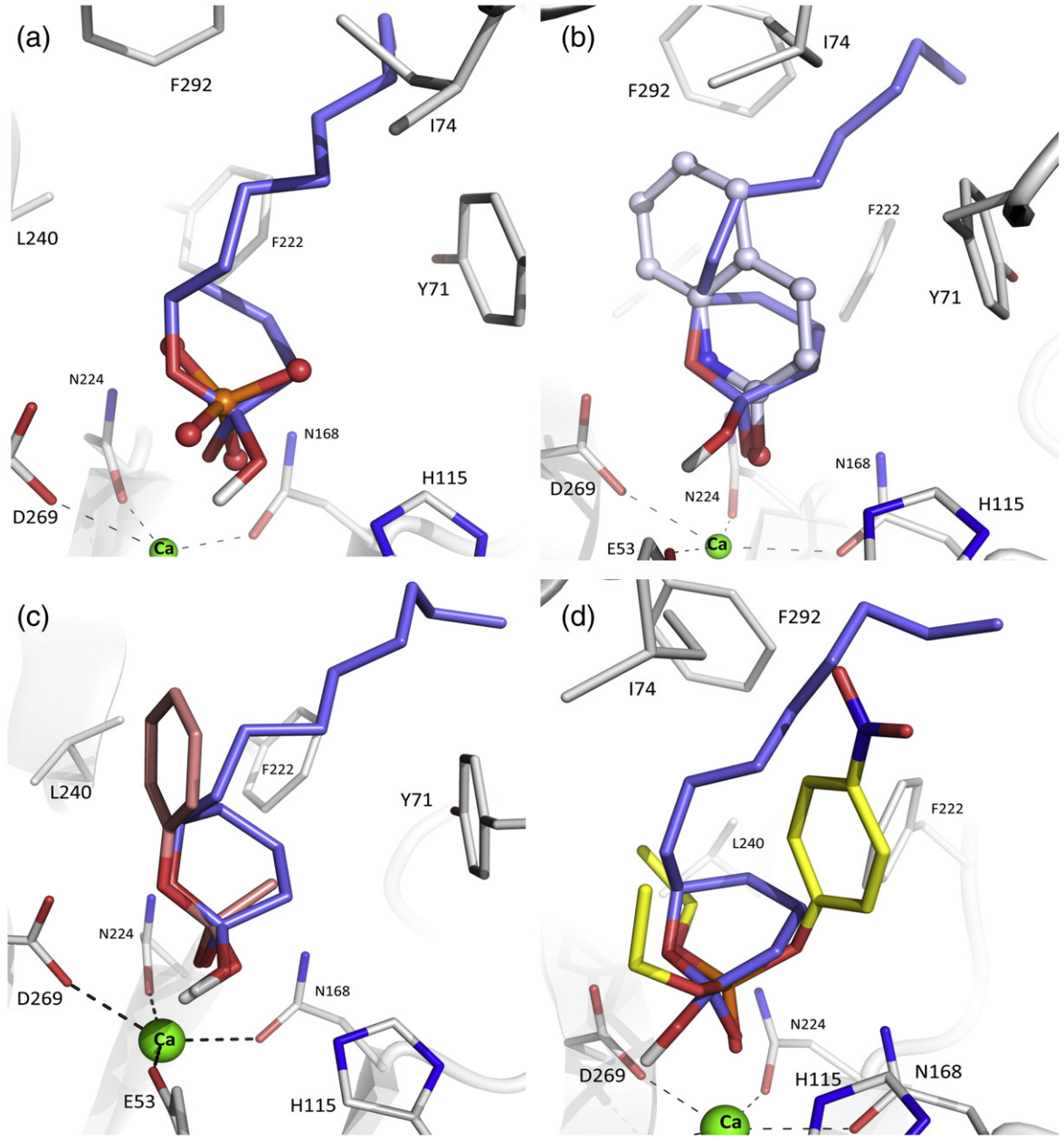

Fig. 6. Superposition of lactone's putative TS with crystal structure ligands and docking models. (a) Superposition of the oxyanion intermediate of *S*-γ-nonanoic lactone (light purple) with the phosphate ion from the actual wild-type pH 6.5 crystal structure (ball and sticks). (b) Superposition of the oxyanion intermediate of *S*-γ-nonanoic lactone (light purple) with the 2HQ from the actual crystal structure of the complex (ball and sticks; light blue). (c) Superposition of the oxyanion intermediate of *S*-γ-nonanoic lactone (light purple) and the reaction intermediate of phenylacetate (pink). (d) Superposition of the oxyanion intermediate of *S*-γ-nonanoic lactone (light purple) and the docking of paraoxon (ground state; in yellow).

carbonyl oxygen is within 1.8–2.1 Å of the catalytic Ca^{2+} (Supplementary Figs. 4a, 5a, and 6c). The putative oxyanionic intermediate suggests that the attacking hydroxide is within bonding distance to both H115 (2.5–3.0 Å) and E53 (2.5–2.7 Å) and at favorable angles (Fig. 8a; Supplementary Figs. 4c and 5c and d). However, for the *R*-isomer, whereas the ground state binds in roughly the same mode as the *S*-isomer (Supplementary Fig. 6a), the corresponding oxyanionic intermediates cannot adopt the same conformations as seen with the intermediates of the *S*-isomers, mainly due to a steric clash

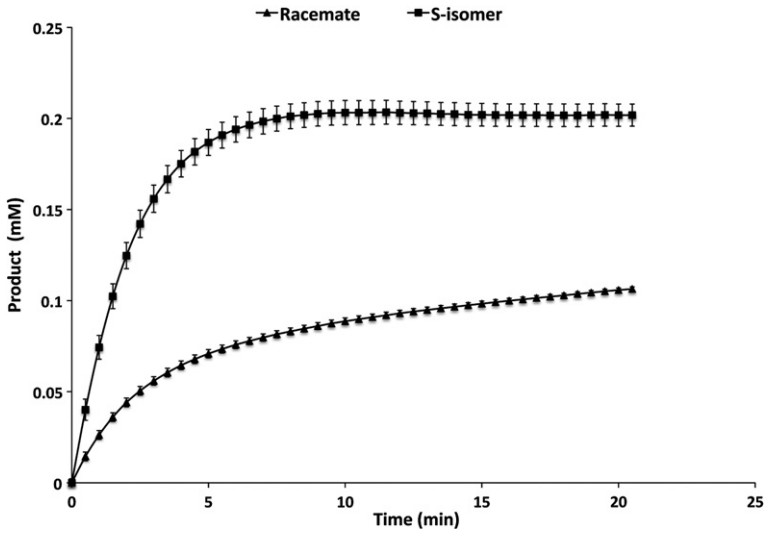

Fig. 7. The course of rePON1 (~1 μM) catalyzed hydrolysis of δ-decanoic thiolactone (0.2 mM), racemate, and the pure *S*-isomer, followed with dithionitrobenzoic acid. Shown is the average of three independent runs. The error bars represent the deviation between these runs. The initial rates (v_0) extracted from these data are as follows: *S*-isomer, 1.14 ± 0.02 μM/s; racemate fast phase, 0.4 ± 0.04 μM/s; and racemate slow phase, 0.023 ± 0.004 μM/s.

with F222 (Supplementary Fig. 8b). The *R*-intermediates thus favor a different binding mode that is likely to result in reduced activity.

Docking of lactones to both the closed and open configurations yielded essentially the same models with respect to the lactone ring orientation. However, in the closed form, two interactions that are not observed in the open form were observed: Y71 contacts the lactone ring, and I74 contacts the alkyl side chain. The substantial decrease in lactonase activity displayed by the Y71A mutant suggests that this activity takes place within the closed conformation. However, the interaction with I74 appears to be less important, since the I74A mutation hardly affects the lactonase activity. Indeed, PON1's structure does not indicate a specific crevice for the alkyl side chain. The aliphatic chain exhibits many degrees of freedom and yields a repertoire of different conformations in the docking simulations. Accordingly, PON1 does not show a strong preference for the size of the alkyl side chain [e.g., γ-caprolactone (ethyl side chain) is hydrolyzed with a k_{cat}/K_m that is only 3-fold lower than that of γ-dodecanoic lactone (heptyl side chain)].[8] Nonetheless, in all the obtained models, the lactone acyl chain interacts with L240 and F292, and mutations of these residues affect PON1's activity with lipophilic lactones.[19] The binding mode of lactones is, therefore, most likely to resemble the model presented in Fig. 8a and in Supplementary Figs. 4a and 5a.

Aryl esters

Phenylacetate is the best known aryl ester substrate of PON1.[8,20–22] It docks to the closed active-site form in a mode that overlaps with 2HQ and phosphate ion in the corresponding crystal structures (Fig. 6). Substrate positioning and the positioning of the corresponding oxyanionic tetrahedral intermediate also resemble those of the *S*-isomers of lactones (Figs. 6c and 8b; Supplementary Fig. 7a and b). Phenylacetate's carbonyl group interacts with the catalytic Ca^{2+} (2.0 Å), and the phenoxide oxygen is positioned similarly to the lactones' alkoxide oxygen. The oxyanionic tetrahedral intermediate is aligned similarly to the ground state (Supplementary Fig. 7c). The attacking hydroxide bridges H115 (2.9 Å) and E53 (2.8 Å), as observed for *S*-isomers of lactones. The phenyl ring resides within a hydrophobic pocket contributed to by V346, I291, F292, L240, F222, and I74. The effect of the I74A mutation (Fig. 5) confirms that I74 is involved in catalysis of phenylacetate. The model also indicates that the methyl group of the acetyl moiety packs against Y71 in the closed structure, and the Y71A mutation decreases phenylacetate activity by ~10-fold (Fig. 5). Thus, although, as found for the lactones, docking of phenylacetate to the open conformations gave binding modes and energies similar to those observed for the closed form, the mutagenesis data suggest that the closed form is most likely to mediate the aryl esterase activity.

The computed models also indicate the proximity of the side chains of I291, F292, and L240 to the phenyl group of phenylacetate. This correlates with aryl esters with para substituents being poor substrates. For example, k_{cat}/K_m for 4-acetoxyacetophenone is >100-fold lower than that for phenylacetate[8] (Supplementary Fig. 7d and e). Furthermore, mutations to smaller residues, for example, F292L/S, I291N, increase activity towards these substrates.[19]

Paraoxon

Unlike aryl esters, which chemically resemble lactones (substrate ambiguity), paraoxon represents a case of catalytic promiscuity (P–O rather the C–O bond cleavage, and a pentavalent, rather than

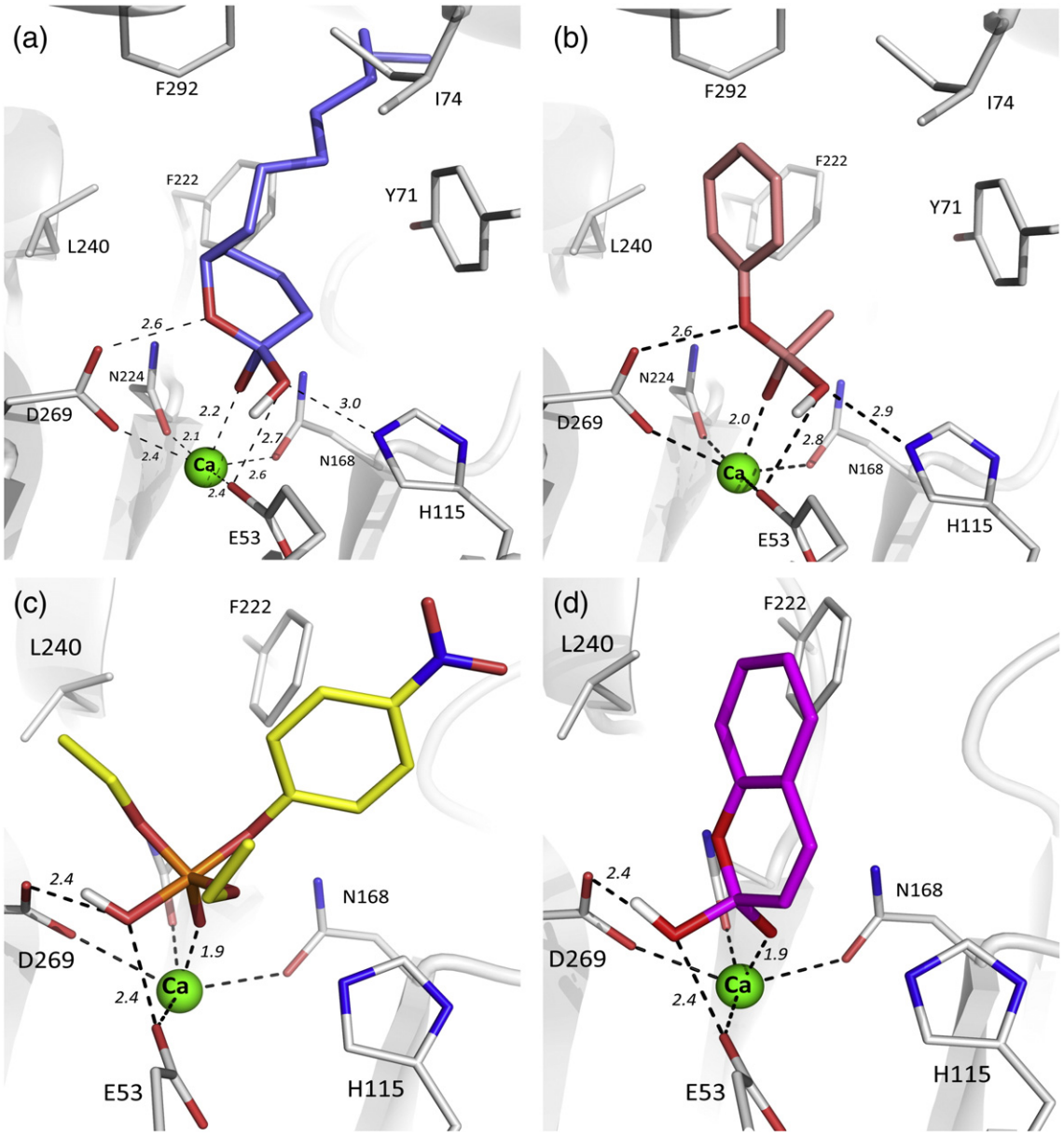

Fig. 8. Docking models of rePON1 with different substrates and their reaction intermediates. (a) PON1's native activity: the oxyanionic tetrahedral intermediate for the hydrolysis of the *S*-isomer of γ-nonanoic lactone within the closed conformation. (b) Substrate ambiguity: the reaction intermediate of phenylacetate hydrolysis within the closed conformation. (c) Catalytic promiscuity: the oxyanionic pentacovalent intermediate of paraoxon hydrolysis within the open conformation. (d) The oxyanion tetrahedral intermediate of dihydrocoumarin hydrolysis within the closed conformation.

tetrahedral, oxyanionic intermediate) (Fig. 1a-c). To unravel the mode of catalysis with paraoxon (and other organophosphates), we attempted to co-crystallize PON1 with various non-hydrolyzable analogues (e.g., phenyl and benzyl, diethyl phosphate, or amidophosphoesters) and with organophosphate substrates while substituting the catalytic calcium by inactive divalent metals ions such as magnesium or strontium. Unfortunately, these attempts were unsuccessful. Either no crystals were obtained or crystals displayed unligated structures. We therefore resorted to docking models validated by the structural and mutational data.

In contrast to the substrates discussed above, paraoxon could not be docked into the closed conformation, not even in a non-catalytic mode. It is simply too voluminous to fit into the closed cavity observed in the 2HQ structure (Supplementary Fig. 8). It docks well, however, in the open conformation (Fig. 8c). The principal residue that prevents the

binding of paraoxon to the closed form is Y71 (Supplementary Fig. 9c). However, paraoxonase activity is significantly reduced when Y71 is mutated to the much smaller Ala (Fig. 5). This suggests that the closed configuration is incompatible with paraoxon hydrolysis not only for steric reasons. Rather, Y71 and I74 (whose mutation to Ala also reduces paraoxonase activity) affect all active-site configurations, including those in which they are not in direct contact with the substrate. We therefore performed docking simulations allowing side-chain flexibility for I74 and Y71. These indicated that the concerted rotation of the side chains of I74 and Y71 enables paraoxon to bind to the closed conformation. However, binding to the catalytic calcium seems weak (3 Å) (Supplementary Fig. 9e and f). It seems, therefore, that paraoxon catalysis is most likely to occur within an open conformation and that the effect of the Y71A and I74A mutations is due to changes in the conformational distribution and not to direct contacts.

The model for the pentavalent oxyanionic intermediate of paraoxon (Fig. 8c, open conformation) is similar to the ground state (Supplementary Fig. 9b). The attacking hydroxide in the pentavalent intermediate interacts with E53 (2.4 Å) and with D269 (2.4 Å) but not with H115, as in the oxyanionic intermediates of *S*-lactones and phenylacetate (Fig. 8a and b). Indeed, mutations in H115 that abolish the lactonase and aryl esterase activities do not affect, or even increase, the paraoxonase activity.[12,13] The docking model for paraoxon is further supported by the observed proximity of one of its ethyl groups to the side chain of V346 (~3.5 Å). Indeed, the V346A mutation increases the k_{cat}/K_m for paraoxon ~10-fold and that for parathiol ~25-fold.[23]

Dihydrocoumarin

Dihydrocoumarin was a challenge for the fidelity of our modeling. It is a lactone, an efficient substrate of PON1 (k_{cat}/K_m of $>10^6$ M^{-1} s^{-1}),[8] and the closest analogue of the lactam inhibitor 2HQ. Nonetheless, whereas catalysis of lactones depends on H115, hydrolysis of dihydrocoumarin is unaffected by mutations of H115.[12] The docking of dihydrocoumarin into both open and closed structures led to similar complexes, and the binding mode is overall similar to that of 2HQ (Supplementary Fig. 10a and b). However, the corresponding oxyanionic tetrahedral intermediate imposes another orientation (Supplementary Fig. 10c), primarily due to steric hindrance with the side chains of F292 and I291. Contrary to the oxyanionic intermediate configurations observed for the *S*-isomers of lipophilic lactones and for phenylacetate, the attacking hydroxide ion in the dihydrocoumarin model displays interactions with E53 (2.4 Å) and D269 (2.5 Å) but not with His115 (Fig. 8d). This mode is very similar to that seen with paraoxon (Fig. 8c; Supplementary Fig. 10d) and is in agreement with mutations of H115 affecting neither dihydrocoumarin nor paraoxon hydrolysis.

Discussion

The structure of PON1 in complex with 2HQ—a competitive lactone analogue inhibitor—provides a first glimpse of the detailed active-site architecture of this enzyme. The flexible 71–81 loop became structured upon binding of 2HQ, thus narrowing the active-site cavity and reshaping its wall. Previous docking and molecular dynamics simulation studies ascribed a role in catalysis for the active-site loop, and for Y71 in particular. However, these were all based on the pH 4.5 structure in which the loop is disordered.[24–27] The structure of the 2HQ complex reveals that the loop adopts a different conformation from those predicted.

The new structures of the 2HQ complex and of apo rePON1 at pH 6.5, and the previously available pH 4.5 structure in complex with a phosphate ion, allowed us to propose detailed models for binding and catalysis of PON1's different substrates and reactions. The models for PON1's native substrates, lactones, and their hydrolytic intermediates relate directly to the mode of binding of 2HQ and phosphate ion, observed in the corresponding crystal structures (Fig. 6a and b). As expected, phenylacetate, which shares the ester reactive group with lactones, shares the same binding mode (Fig. 6c). The derived models of the tetrahedral oxyanionic intermediates are further supported by the newly discovered preference of PON1 for the *S*-enantiomers of lactone substrates (Fig. 7).

The detailed models derived here support the previously proposed lactonase mechanism, but they do reveal a significant difference. The attacking hydroxide seems to interact not only with H115, as previously proposed,[12] but also with E53. The latter is a calcium-ligating residue, and its role beyond binding the catalytic calcium is therefore hard to establish. As is the case with another calcium-ligating residue, D269,[12] a site saturation library of E53 in which Glu was substituted by the other 19 amino acids revealed that all mutations at this position resulted in loss of activity, at least at the level that can be detected in crude lysates. However, support for the notion that E53 might also be involved in generating the attacking hydroxide comes from the structure of a glucuronolactonase from *Xanthomonas campestris* (PDB ID: 3DR2).[28] This enzyme has an Asn at position 115 rather than His, as in PON1. However, E48, the calcium-binding

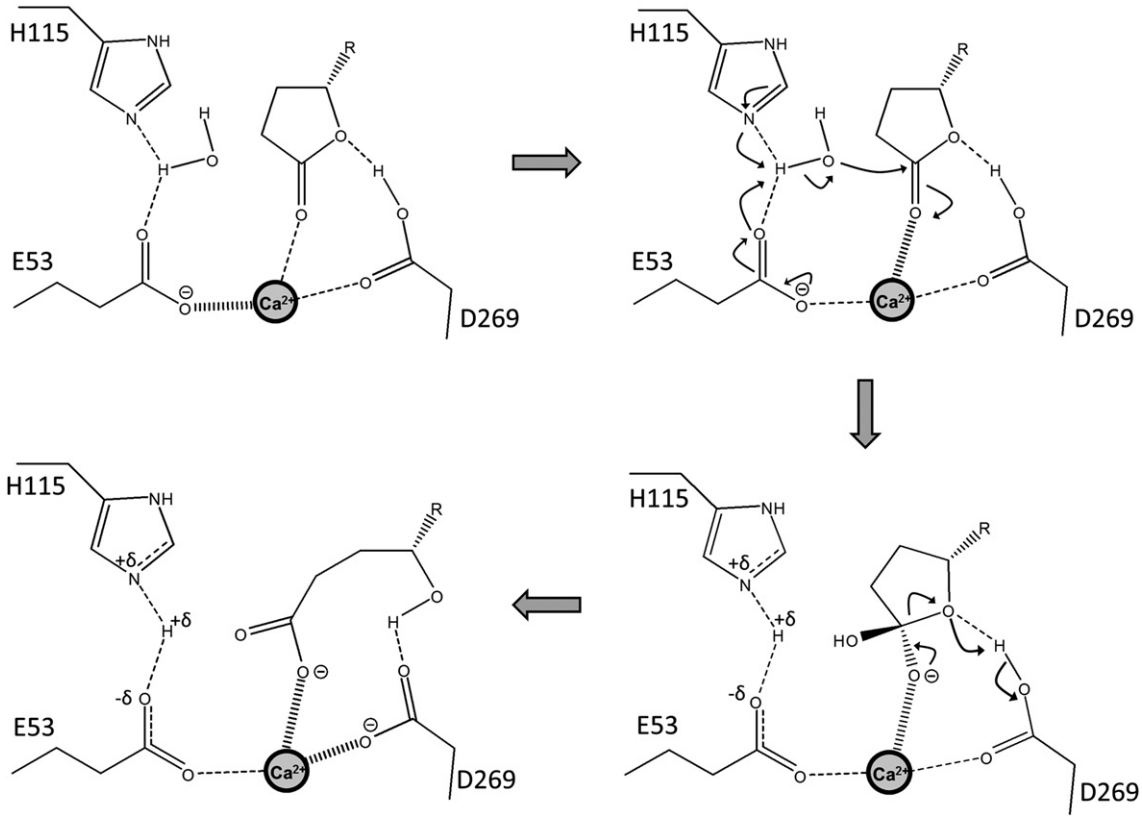

Fig. 9. The proposed mechanism for the hydrolysis of lactones by rePON1. The same mechanism applies to the aryl esterase activity. Note the proposed charge relay between the reaction intermediate, the calcium atom, and its ligating residues depicted by wide and narrow broken lines. Deprotonation of the water and the concomitant protonation of E53 weaken E53's interaction with the calcium and may thereby enable further stabilization of the negatively charged oxyanion intermediate. The reverse charge flow may apply to the leaving-group protonation and D269, although the evidence for the latter's role as general acid is indirect (see the text).

residue that corresponds to PON1's Glu53, adopts different conformations in each of the two molecules of the asymmetric unit. One conformation is PON1-like, with E48 interacting directly with the calcium cation. In the second conformation, however, a water molecule bridges E48 and the calcium ion. The bond between E48 and the water molecule is notably short (2.5 Å), supporting a role in catalysis (Supplementary Fig. 11). Participation of metal-ligating residues in the alignment and/or activation of the attacking water molecule has been documented for other metallo-hydrolases.[29–31] Thus, we surmise that PON1's lactonase activity is mediated by a hydroxide nucleophile that is generated *via* general base catalysis by both H115 and E53, with the latter also ligating the catalytic calcium (Fig. 9). The same mechanism applies to the aryl esterase activity.

Comparison of the 2HQ complex and of the substrate docking models also suggests a potential role for D269. Its side-chain carboxyl appears to form an H-bond, with the amide NH of 2HQ serving as the donor. But, the corresponding ester group of lactone substrates can only act as an acceptor. However, in its protonated form, D269 can form an H-bond with lactones and thus facilitate the protonation of the alkoxide leaving group. The Brønsted leaving-group plots for PON1 are complex; nevertheless, the lactonase and aryl esterase activities show little sensitivity to the pK_a of the leaving group, thus suggesting involvement of general acid catalysis.[8] D269 is the most likely candidate for this role. Indeed, in the structurally and functionally related enzyme *Staphylococcus aureus* Drp35, D236 (equivalent to D269 in PON1) was hypothesized to be protonated, thus facilitating leaving-group protonation.[32]

Phenylacetate fits the expected mode for substrate ambiguity. Although it is an aryl ester, it binds in a similar fashion to lactones and utilizes the same catalytic mechanism (Figs. 6c and 9). We also observed that minor structural alterations in promiscuous substrates such as aryl esters and phosphotriesters may severely reduce the turnover rate (e.g., para substituents in aryl esters). In

contrast, differences between closely related lactone substrates are primarily manifested in different K_m values.[8] As also indicated by the docking models, suboptimal lactone substrates bind with weaker affinity, but the transition state is correctly positioned. In contrast, the promiscuous substrates seem to bind with the same affinity (~1 mM K_m values[8]), but some substrates show suboptimal positioning relative to the catalytic residues, thus accounting for their very low k_{cat} values (Supplementary Fig. 7d).

Paraoxon represents a case of catalytic promiscuity—hydrolysis of a P–O bond by an enzyme whose native activity is hydrolysis of C–O bonds (Fig. 1). Unlike for the lactones and aryl esters, where 2HQ and phosphate serve as suitable analogues, the proposed catalytic mode for paraoxon was derived from docking only. Nonetheless, the models seem to be in agreement with the mutational data. The models suggest that paraoxon's phosphoryl oxygen and the oxygen of one of its ethyl ester groups overlap with the lactone's ester group in its tetrahedral, oxyanionic intermediate (Fig. 6d; Supplementary Fig. 7c). Thus, the promiscuous paraoxonase activity seems to stem from a coincidental overlap between paraoxon and the intermediate state (and corresponding transition states) for the native lactonase activity. The correct alignment of paraoxon *versus* the catalytic calcium and the presence of residues that mediate water activation result in the hydrolytic breakdown of paraoxon rather than in binding. This overlap stems from the lactone's cyclic geometry and seems to be the key prerequisite for PON1's catalytic promiscuity. Notably, this overlap also appears to be a general theme that occurs with enzymes of different folds and superfamilies.[33] It may therefore permit the prediction of promiscuous sites. Although challenging, predicting promiscuous enzymes for a given reaction is of great potential in biocatalysis and enzyme engineering. Such prediction may be performed by virtual docking,[16,34,35] guided by the analogy between promiscuous substrates and synthetic inhibitors. The binding of human-made enzyme inhibitors is promiscuous (no enzyme evolved to bind its inhibitor). Nonetheless, inhibitors that bear no apparent structural resemblance to the native substrate often recapitulate key interactions within the enzyme's active site,[36,37] as is seen here for promiscuous substrates (Fig. 6c and d).

However, this overlap is also enabled by the existence of multiple active-site configurations. The closed conformation that is highly complementary to the lactones' hydrolytic intermediates is incompatible with the binding of paraoxon in a catalytically relevant mode. Rather, the open conformation, in which Y71 is flipped out and the rest of the loop residues are likely to be disordered, accommodates paraoxon. It should be noted, however, that promiscuity depends on maintaining key interactions with the active site's catalytic residues. Whether binding of a promiscuous substrate in a manner that takes advantage of these key interactions occurs within the same active-site conformation used by the native substrate, or within a different one, is purely a matter of coincidence.

What remains unclear despite many studies is the identity of the attacking nucleophile for paraoxon hydrolysis. It could be an active-site residue (the models indicate that D269 and E53 are appropriately positioned) or a water molecule activated by either or both of these two residues.[12,25,27,38,39] Pre-steady-state kinetics that we performed indicated linear rates with paraoxon, as well as with its activated derivative, 2,4-dinitrophenyl-diethylphosphate (O. Khersonsky, personal communication). The most parsimonious explanation for the absence of burst kinetics is that water is the attacking nucleophile. Our model suggests that the attacking water is indeed aligned and activated by E53 and D269. However, because these residues are absolutely essential for ligating the catalytic Ca^{2+}, their additional roles in catalysis are hard to decipher since mutations in these residues result in non-detectable activity (as shown here for E53, and for D269 in Ref. 12). In any case, H115, which is required for water activation in lactones hydrolysis, is absolutely unnecessary for paraoxonase activity.

In contrast to phenylacetate, dihydrocoumarin constitutes an unexpected deviation from the anticipated mode of substrate ambiguity. Although it is a lactone, both the docking models, and the absence of effect of H115 mutations,[12] support a mode of catalysis that resembles that of paraoxon (catalytic promiscuity) rather than of phenylacetate (substrate ambiguity). Dihydrocoumarin thus demonstrates how complex enzyme active sites may be and how multiple modes of action are afforded when several residues with catalytic potential are adjacent to each other.

In summary, the multiple substrate binding modes and reaction mechanisms unraveled by this study show three underlining themes:

(1) Coincidental overlaps between the transition state (and/or the reactive intermediate) for the native reaction and the ground state and/or transition states for promiscuous substrates and reactions (Fig. 6c and d).
(2) Conformational diversity afforded primarily by the active-site loop (including backbone and side-chain flexibility) that permits alternative active-site configurations, which, in turn, bind and process different substrates. Proteins

are intrinsically dynamic and, as a consequence, sample a large number of different conformations. The existence of multiple conformational subsets may also allow binding and catalysis of non-native substrates, thus giving rise to alternative and promiscuous functions.[2–6,40,41]

(3) The third theme that we observed is a network of catalytic residues and reaction coordinates within PON1's active site. This network provides both backup and evolutionary versatility. H115 is responsible for generating the attacking hydroxide. However, H115 does not act on its own, but in conjunction with other residues: E53 and H134, which comprises part of the His dyad of PON1.[12] Indeed, mutating H115 to Gln, which is similar in size and hydrogen-bonding potential but ineffective as a base, reduces the lactonase activity by only ~20- to 100-fold depending on the substrate. This is no exception: mutations in key active-site residues often result in mild effects, but the reasons for this phenomenon remain unclear.[42] This case study indicates that beyond the catalytic calcium that comprises the essential, central piece of PON1's active site, there exists a network of multiple overlapping active-site residues that mediate individual catalytic steps. Specifically, the catalytic calcium and its ligating residues comprise a highly networked environment. The positively charged calcium acts as an oxyanion hole, yet the surrounding ligands are negatively charged and can act as either base or acid depending on their protonation state. The ligating residues can therefore assist in aligning and activating water for the nucleophilic attack or in protonating the leaving group, as seen in many other metallo-enzymes.[43–45] Removal of an individual residue, such as His115, affects catalysis but does not abolish it altogether—primarily because other residues in the catalytic network take over the role of H115. This catalytically rich environment also mediates PON1's catalytic promiscuity. By utilizing different parts of this extensive network of catalytic and auxiliary residues, PON1 catalyzes reactions such as paraoxon or dihydrocoumarin hydrolysis in a mode that differs from that of the native lactonase activity. In other words (borrowed from an anonymous reviewer's report on this article), enzyme active sites present a manifold of multiple reaction coordinates, one of which is optimal and is followed by the native activity. However, other coordinates may be promiscuously available, even though they are higher in energy and therefore result in low rate accelerations.

The network arrangement of active sites might also be the key to their evolvability. Two cases of natural paraoxonases that diverged from bacterial metallolactonases with promiscuous organophosphate hydrolase activity are already known. Remarkably, this divergence occurred within a few decades and yielded highly efficient enzymes.[33,46,47] In the case of PON1, laboratory evolution indicated that mutations of H115 direct the evolution of proficient organophosphate hydrolases.[48] The structural models presented here suggest that this change occurs *via* a subtle shift such that E53, possibly together with D269, activates the nucleophilic water, instead of H115 together with E53. Similar shifts within the active-site networks of other lactonases are likely to have facilitated their divergence, thus yielding highly proficient paraoxonases within a few decades.

Materials and Methods

rePON1 variants

Expression and purification of rePON1–G2E6 and its mutants were performed as previously described[11] with minor changes. Briefly, the Ni-NTA step was followed by an ion-exchange chromatography step during which the detergent was changed from 0.1% Tergitol to 0.03% *n*-dodecyl-β-D-maltoside. The purest fractions were pooled and incubated at 25 °C for 10 days or at room temperature overnight in the presence of thrombin (~1 U/mg protein), to promote cleavage of the thioredoxin tag. The tag-free PON1 was purified on Superdex G-200. RePON1–G2E6 was also used as the template for generating the alanine mutants using 'inverse PCR'.[12] The mutated genes were verified by DNA sequencing, and the enzyme variants were purified by Ni-NTA. The purity of rePON1–G2E6 and of its mutants was monitored by SDS-PAGE. The glutamate (E53) site saturation library was generated by replacing Glu codons with NNS codons (where N is a mixture of all four nucleotides and S is a mixture of C and G) encoding all amino acids.

Kinetics

Kinetic measurements, using paraoxon (phosphotriesterase activity), TBBL (4-Thiobutyl γ-butyrolactone; lactonase activity), and phenylacetate (esterase activity) as substrates, were performed as previously described[12] (Fig. 1). Substrate concentrations were in the range of $0.3 \times K_m$ up to $(2–3) \times K_m$. k_{cat}, K_m, and k_{cat}/K_m were obtained by fitting the data to the Michaelis–Menten model with PRISM (GraphPad Software). In cases in which substrate solubility was limiting, k_{cat}/K_m values were extracted from linear fits. All data presented are the mean obtained from ≥2 independent experiments, and the error ranges represent the standard deviation from the mean.

Crystallization, data collection, and refinement

Concentrated solutions of rePON1–G2E6 (5–10 mg/ml) were subjected to crystallization trials. The best crystals

were obtained in 20% polyethylene glycol 3350/0.2 M NaBr/0.1 M 2-[bis(2-hydroxyethyl)amino]-2-(hydroxymethyl)propane-1,3-diol propane, pH 6.5, at 19 °C. A 20-mM solution of 2HQ in dimethyl sulfoxide was used for both the co-crystallization and soaking-in experiments (yielding a final 1–5 mM 2HQ concentration in the drop). Complete data sets for rePON1 and 2HQ/rePON1 were collected on beamlines ID-29 and ID-14-4, respectively, at the European Synchrotron Radiation Facility (Grenoble, France). The diffraction images were indexed, integrated, and scaled using the HKL2000 program package.[49] Structure determination was carried out by molecular replacement (Phaser, CCP4[50]) using the published pH 4.5 structure (PDB ID: 1V04) as the starting model for the ligand-free structure at pH 6.5 and the latter for refining the structure of the 2HQ complex. All steps of atomic refinement were carried out with CCP4/Refmac5.[51] The model was built into $2F_o-F_c$ and F_o-F_c maps using the program Coot.[52] Both the ligand-free rePON1 and the 2HQ complex did not display well-defined electron density for the first ~20 residues at the N-terminus, as had already been observed for 1V04. Both structures contain one molecule of *n*-dodecyl-β-D-maltoside (with density corresponding to the sugar moiety). Details of data collection and refinement statistics are displayed in Table 1. Figures depicting structures were prepared using PyMOL.[53]

Molecular docking

Ligand coordinates were generated using *Jligand*† and the DockingServer‡. The torsion and charge parameters were generated using ADT 4.2§ and the Gasteiger method, with the exception of the hydrolysis intermediates, where a single negative charge was attributed to the oxyanion atom. Hydrogen atom positions of the receptor protein models were added using ADT 4.2. The atomic partial charges of the receptor protein models were assigned using ADT 4.2 and the Gasteiger method. A +2 charge was attributed to the two calcium ions. The docking simulations were performed using Autodock 4.0[54,55] and the Lamarckian genetic algorithm. Thirty runs of genetic algorithm were performed for each ligand–receptor pair using the default parameters. The output ligand configurations were clustered and selected by their binding energy scores and chemical relevance.

Accession numbers

Coordinates and structure factors of the wild-type rePON1 at pH 6.5 and of its complex with 2HQ have been deposited in the PDB under accession numbers 3SRE and 3SRG, respectively. An Interactive 3D Complement (I3DC) page appears in Proteopedia for this study‖.

† http://www.ysbl.york.ac.uk/mxstat/JLigand/index.html
‡ http://www.dockingserver.com
§ http://autodock.scripps.edu/resources/adt
‖ http://proteopedia.org/w/Journal:JMB:2

Acknowledgements

We thank the Israel Structural Proteomics Centre for access to their protein purification and crystallization facilities and Marcin Suskiewicz for his valuable assistance in the kinetic measurements. M.E. is a fellow supported by the Intra-European Fellowship Marie Curie program (grant no. 252836). Financial support by the National Institutes of Health (2-U54-NS058183), the Defense Threat Reduction Agency (HDTRA1-11-C-0026), and the Benoziyo Center for Neuroscience is gratefully acknowledged. D.S.T. is the Nella and Leon Benoziyo Professor of Biochemistry. J.L.S. is the Pickman Professor of Structural Biology. We are very grateful to Reviewer #2 for his or her inspirational comments.

Supplementary Data

Supplementary data associated with this article can be found, in the online version, at doi:10.1016/j.jmb.2012.02.042

References

1. Khersonsky, O. & Tawfik, D. S. (2010). Enzyme promiscuity: a mechanistic and evolutionary perspective. *Annu. Rev. Biochem.* **79**, 471–505.
2. Hou, L., Honaker, M. T., Shireman, L. M., Balogh, L. M., Roberts, A. G., Ng, K. C. *et al.* (2007). Functional promiscuity correlates with conformational heterogeneity in A-class glutathione *S*-transferases. *J. Biol. Chem.* **282**, 23264–23274.
3. Li, B., Sher, D., Kelly, L., Shi, Y., Huang, K., Knerr, P. J. *et al.* (2010). Catalytic promiscuity in the biosynthesis of cyclic peptide secondary metabolites in planktonic marine cyanobacteria. *Proc. Natl Acad. Sci. USA*, **107**, 10430–10435.
4. Lu, X., Li, L., Wu, R., Feng, X., Li, Z., Yang, H. *et al.* (2006). Kinetic analysis of *Pseudomonas aeruginosa* arginine deiminase mutants and alternate substrates provides insight into structural determinants of function. *Biochemistry*, **45**, 1162–1172.
5. Theodossis, A., Walden, H., Westwick, E. J., Connaris, H., Lamble, H. J., Hough, D. W. *et al.* (2004). The structural basis for substrate promiscuity in 2-keto-3-deoxygluconate aldolase from the Entner–Doudoroff pathway in *Sulfolobus solfataricus*. *J. Biol. Chem.* **279**, 43886–43892.
6. Yasutake, Y., Yao, M., Sakai, N., Kirita, T. & Tanaka, I. (2004). Crystal structure of the *Pyrococcus horikoshii* isopropylmalate isomerase small subunit provides insight into the dual substrate specificity of the enzyme. *J. Mol. Biol.* **344**, 325–333.
7. Draganov, D. I., Teiber, J. F., Speelman, A., Osawa, Y., Sunahara, R. & La Du, B. N. (2005). Human paraoxonases (PON1, PON2, and PON3) are lactonases with overlapping and distinct substrate specificities. *J. Lipid Res.* **46**, 1239–1247.

8. Khersonsky, O. & Tawfik, D. S. (2005). Structure-reactivity studies of serum paraoxonase PON1 suggest that its native activity is lactonase. *Biochemistry*, **44**, 6371–6382.
9. Fishbein, W. N. & Bessman, S. P. (1966). Purification and properties of an enzyme in human blood and rat liver microsomes catalyzing the formation and hydrolysis of gamma-lactones. II. Metal ion effects, kinetics, and equilibria. *J. Biol. Chem.* **241**, 4842–4847.
10. Fishbein, W. N. & Bessman, S. P. (1966). Purification and properties of an enzyme in human blood and rat liver microsomes catalyzing the formation and hydrolysis of gamma-lactones. I. Tissue localization, stoichiometry, specificity, distinction from esterase. *J. Biol. Chem.* **241**, 4835–4841.
11. Harel, M., Aharoni, A., Gaidukov, L., Brumshtein, B., Khersonsky, O., Meged, R. *et al.* (2004). Structure and evolution of the serum paraoxonase family of detoxifying and anti-atherosclerotic enzymes. *Nat. Struct. Mol. Biol.* **11**, 412–419.
12. Khersonsky, O. & Tawfik, D. S. (2006). The histidine 115–histidine 134 dyad mediates the lactonase activity of mammalian serum paraoxonases. *J. Biol. Chem.* **281**, 7649–7656.
13. Yeung, D. T., Lenz, D. E. & Cerasoli, D. M. (2005). Analysis of active-site amino-acid residues of human serum paraoxonase using competitive substrates. *FEBS J.* **272**, 2225–2230.
14. Aharoni, A., Gaidukov, L., Yagur, S., Toker, L., Silman, I. & Tawfik, D. S. (2004). Directed evolution of mammalian paraoxonases PON1 and PON3 for bacterial expression and catalytic specialization. *Proc. Natl Acad. Sci. USA*, **101**, 482–487.
15. Billecke, S., Draganov, D., Counsell, R., Stetson, P., Watson, C., Hsu, C. & La Du, B. N. (2000). Human serum paraoxonase (PON1) isozymes Q and R hydrolyze lactones and cyclic carbonate esters. *Drug Metab. Dispos.* **28**, 1335–1342.
16. Hermann, J. C., Marti-Arbona, R., Fedorov, A. A., Fedorov, E., Almo, S. C., Shoichet, B. K. & Raushel, F. M. (2007). Structure-based activity prediction for an enzyme of unknown function. *Nature*, **448**, 775–779.
17. Chapman, E. & Wong, C. H. (2002). A pH sensitive colorometric assay for the high-throughput screening of enzyme inhibitors and substrates: a case study using kinases. *Bioorg. Med. Chem.* **10**, 551–555.
18. Filippi, J. J., Fernandez, X. & Dunach, E. (2006). Lewis acid-catalysed isomerisation of thionolactones to thiolactones: inversion of configuration. *Tetrahedron Lett.* **47**, 6067–6070.
19. Gupta, R. D. & Tawfik, D. S. (2008). Directed enzyme evolution via small and effective neutral drift libraries. *Nat. Methods*, **5**, 939–942.
20. Draganov, D. I. & La Du, B. N. (2004). Pharmacogenetics of paraoxonases: a brief review. *Naunyn-Schmiedeberg's Arch. Pharmacol.* **369**, 78–88.
21. Gan, K. N., Smolen, A., Eckerson, H. W. & La Du, B. N. (1991). Purification of human serum paraoxonase/arylesterase. Evidence for one esterase catalyzing both activities. *Drug Metab. Dispos.* **19**, 100–106.
22. Teiber, J. F., Draganov, D. I. & La Du, B. N. (2004). Purified human serum PON1 does not protect LDL against oxidation in the in vitro assays initiated with copper or AAPH. *J. Lipid Res.* **45**, 2260–2268.
23. Amitai, G., Gaidukov, L., Adani, R., Yishay, S., Yacov, G., Kushnir, M. *et al.* (2006). Enhanced stereoselective hydrolysis of toxic organophosphates by directly evolved variants of mammalian serum paraoxonase. *FEBS J.* **273**, 1906–1919.
24. Fairchild, S. Z., Peterson, M. W., Hamza, A., Zhan, C. G., Cerasoli, D. M. & Chang, W. E. (2010). Computational characterization of how the VX nerve agent binds human serum paraoxonase 1. *J. Mol. Model.* **17**, 97–109.
25. Hu, X., Jiang, X., Lenz, D. E., Cerasoli, D. M. & Wallqvist, A. (2009). In silico analyses of substrate interactions with human serum paraoxonase 1. *Proteins*, **75**, 486–498.
26. Peterson, M. W., Fairchild, S. Z., Otto, T. C., Mohtashemi, M., Cerasoli, D. M. & Chang, W. E. (2011). VX hydrolysis by human serum paraoxonase 1: a comparison of experimental and computational results. *PLoS One*, **6**, e20335.
27. Sanan, T. T., Muthukrishnan, S., Beck, J. M., Tao, P., Hayes, C. J., Otto, T. C. *et al.* (2010). Computational modeling of human paraoxonase 1: preparation of protein models, binding studies, and mechanistic insights. *J. Phys. Org. Chem.* **23**, 357–369.
28. Chen, C. N., Chin, K. H., Wang, A. H. & Chou, S. H. (2008). The first crystal structure of gluconolactonase important in the glucose secondary metabolic pathways. *J. Mol. Biol.* **384**, 604–614.
29. Aubert, S. D., Li, Y. & Raushel, F. M. (2004). Mechanism for the hydrolysis of organophosphates by the bacterial phosphotriesterase. *Biochemistry*, **43**, 5707–5715.
30. Momb, J., Wang, C., Liu, D., Thomas, P. W., Petsko, G. A., Guo, H. *et al.* (2008). Mechanism of the quorum-quenching lactonase (AiiA) from *Bacillus thuringiensis*. 2. Substrate modeling and active site mutations. *Biochemistry*, **47**, 7715–7725.
31. Elias, M., Dupuy, J., Merone, L., Mandrich, L., Porzio, E., Moniot, S. *et al.* (2008). Structural basis for natural lactonase and promiscuous phosphotriesterase activities. *J. Mol. Biol.* **379**, 1017–1028.
32. Tanaka, Y., Morikawa, K., Ohki, Y., Yao, M., Tsumoto, K., Watanabe, N. *et al.* (2007). Structural and mutational analyses of Drp35 from *Staphylococcus aureus*: a possible mechanism for its lactonase activity. *J. Biol. Chem.* **282**, 5770–5780.
33. Elias, M. & Tawfik, D. S. (2012). Divergence and convergence in enzyme evolution: parallel evolution of paraoxonases from quorum-quenching lactonases. *J. Biol. Chem.* **287**, 11–20.
34. Kalyanaraman, C., Bernacki, K. & Jacobson, M. P. (2005). Virtual screening against highly charged active sites: identifying substrates of alpha-beta barrel enzymes. *Biochemistry*, **44**, 2059–2071.
35. Shoichet, B. K. (2004). Virtual screening of chemical libraries. *Nature*, **432**, 862–865.
36. Powers, R. A., Morandi, F. & Shoichet, B. K. (2002). Structure-based discovery of a novel, noncovalent inhibitor of AmpC beta-lactamase. *Structure*, **10**, 1013–1023.
37. Vaaje-Kolstad, G., Vasella, A., Peter, M. G., Netter, C., Houston, D. R., Westereng, B. *et al.* (2004). Interactions of a family 18 chitinase with the designed inhibitor HM508 and its degradation product, chitobiono-delta-lactone. *J. Biol. Chem.* **279**, 3612–3619.

38. Blum, M. M., Lohr, F., Richardt, A., Ruterjans, H. & Chen, J. C. (2006). Binding of a designed substrate analogue to diisopropyl fluorophosphatase: implications for the phosphotriesterase mechanism. *J. Am. Chem. Soc.* **128**, 12750–12757.
39. Blum, M. M. & Chen, J. C. (2010). Structural characterization of the catalytic calcium-binding site in diisopropyl fluorophosphatase (DFPase)—comparison with related beta-propeller enzymes. *Chem. Biol. Interact.* **187**, 373–379.
40. Boehr, D. D., Nussinov, R. & Wright, P. E. (2009). The role of dynamic conformational ensembles in biomolecular recognition. *Nat. Chem. Biol.* **5**, 789–796.
41. Tokuriki, N. & Tawfik, D. S. (2009). Protein dynamism and evolvability. *Science*, **324**, 203–207.
42. Peracchi, A. (2001). Enzyme catalysis: removing chemically 'essential' residues by site-directed mutagenesis. *Trends Biochem. Sci.* **26**, 497–503.
43. Cotton, F. A., Hazen, E. E., Jr. & Legg, M. J. (1979). Staphylococcal nuclease: proposed mechanism of action based on structure of enzyme–thymidine 3′,5′-bisphosphate–calcium ion complex at 1.5-Å resolution. *Proc. Natl Acad. Sci. USA*, **76**, 2551–2555.
44. Essen, L. O., Perisic, O., Katan, M., Wu, Y., Roberts, M. F. & Williams, R. L. (1997). Structural mapping of the catalytic mechanism for a mammalian phosphoinositide-specific phospholipase C. *Biochemistry*, **36**, 1704–1718.
45. Xie, F., Briggs, J. M. & Dupureur, C. M. (2010). Nucleophile activation in PD...(D/E)xK metallonucleases: an experimental and computational p*K*(a) study. *J. Inorg. Biochem.* **104**, 665–672.
46. Dong, Y. J., Bartlam, M., Sun, L., Zhou, Y. F., Zhang, Z. P., Zhang, C. G. *et al.* (2005). Crystal structure of methyl parathion hydrolase from *Pseudomonas* sp. WBC-3. *J. Mol. Biol.* **353**, 655–663.
47. Omburo, G. A., Kuo, J. M., Mullins, L. S. & Raushel, F. M. (1992). Characterization of the zinc binding site of bacterial phosphotriesterase. *J. Biol. Chem.* **267**, 13278–13283.
48. Gupta, R. D., Goldsmith, M., Ashani, Y., Simo, Y., Mullokandov, G., Bar, H. *et al.* (2011). Directed evolution of hydrolases for prevention of G-type nerve agent intoxication. *Nat. Chem. Biol.* **7**, 120–125.
49. Otwinowski, Z. & Minor, W. (1997). Processing of X-ray diffraction data collected in oscillation mode. *Methods Enzymol.* **276**, 307–326.
50. McCoy, A. J., Grosse-Kunstleve, R. W., Adams, P. D., Winn, M. D., Storoni, L. C. & Read, R. J. (2007). Phaser crystallographic software. *J. Appl. Crystallogr.* **40**, 658–674.
51. Murshudov, G. N., Vagin, A. A. & Dodson, E. J. (1997). Refinement of macromolecular structures by the maximum-likelihood method. *Acta Crystallogr., Sect. D: Biol. Crystallogr.* **53**, 240–255.
52. Emsley, P. & Cowtan, K. (2004). Coot: model-building tools for molecular graphics. *Acta Crystallogr., Sect. D: Biol. Crystallogr.* **60**, 2126–2132.
53. DeLano, W. L. (2002). *The PyMOL Molecular Graphics System.* DeLano Scientific LLC, San Carlos, CA. http://www.pymol.org.
54. Huey, R., Morris, G. M., Olson, A. J. & Goodsell, D. S. (2007). A semiempirical free energy force field with charge-based desolvation. *J. Comput. Chem.* **28**, 1145–1152.
55. Morris, G. M., Goodsell, D. S., Halliday, R. S., Huey, R., Hart, W. E., Belew, R. K. & Olson, A. J. (1998). Automated docking using a Lamarckian genetic algorithm and an empirical binding free energy function. *J. Comput. Chem.* **19**, 1639–1662.